Bifurcation and scaling of drift wave turbulence intensity with collisional zonal flow damping

M. A. Malkov and P. H. Diamond

Citation: Physics of Plasmas **8**, 3996 (2001); doi: 10.1063/1.1394760
View online: http://dx.doi.org/10.1063/1.1394760
View Table of Contents: http://scitation.aip.org/content/aip/journal/pop/8/9?ver=pdfcov
Published by the AIP Publishing

Bifurcation and scaling of drift wave turbulence intensity with collisional zonal flow damping

M. A. Malkov[a] and P. H. Diamond
University of California at San Diego, 9500 Gilman Dr., La Jolla, California 92093-0319

(Received 21 March 2001; accepted 22 June 2001)

Interacting drift wave–zonal flow turbulence is examined at the spectral level of description using an extended ''predator–prey'' model. Analytic solutions that describe both the linear scaling of transport with ion–ion collisionality as well as the saturation regime are obtained for a simple model of drift wave turbulence. A theory of self-regulation in this system is presented. The possibility of bifurcation to a state with higher turbulence level and transport is demonstrated. This bifurcation is associated with the appearance of a condensate solution at the largest scales. The possible relevance of this phenomenon to the bursting events of turbulence and transport recently observed in gyrokinetic simulations of ITG instability is discussed. © *2001 American Institute of Physics.* [DOI: 10.1063/1.1394760]

I. INTRODUCTION

The mechanisms for generation of fluid motions with additional symmetry, frequently referred to as flows (both mean and zonal), have been extensively studied in many astrophysical, geophysical, and laboratory settings. Examples range from the Jovian belt-type flows and the rapid rotation of the Venusian atmosphere (60 times faster than the planet itself), to the $\mathbf{E}\times\mathbf{B}$ flow layers in magnetic confinement devices. The common element of these mechanisms is the Reynolds stress $\langle u'v'\rangle$, where the primed variables stand for the velocity perturbations along the flow (y) and cross-stream (x) directions. In the framework of the Navier–Stokes equation, Reynolds stress drive may be balanced by the viscous stress of the generated shear, $\nu d\langle v\rangle/dx$, or by different dissipation mechanisms in other models. The velocity perturbations can be due to externally induced symmetry breaking. Perhaps the most straightforward example of this is the so-called ''moving flame mechanism'' suggested to explain the strong zonal wind in the Venusian atmosphere (e.g., Ref. 1). Under certain circumstances, the convective motion generated by a periodic heat source (the Sun) in motion along the Equator has a nonzero Reynolds stress that produces a mean flow. This is an example of a direct Reynolds stress generation by forcing. The second type of symmetry breaking is thought to be responsible for the generation of zonal winds on major planets Jupiter and Saturn. It is based on the secondary instability of the thermally driven Rossby waves that generate a zonal flow perpendicular to the heat flux. This flow has the remarkable property that it reduces the turbulent thermal flux, so that the latter decreases with increasing Rayleigh number (Refs. 2–7). The efficiency of this reduction is evidently determined by the branching ratio of the instability free energy (originally deposited in the temperature or density gradient, etc.) between the symmetric $(k_y=0)$ component of turbulence and its nonsymmetric $(k_y\neq 0)$ component, which drives a heat flux.

Studies of gradient instabilities in fluids and plasmas have profited from the well-known Rossby–drift wave duality. Therefore the phenomenon of turbulence reduction is to be expected in magnetic confinement devices, a topic which is of great interest to the fusion program. There is indeed compelling evidence of this transport regulating mechanism in tokamak plasmas. It was demonstrated by gyrofluid[8–10] and gyrokinetic[11–14] simulations as well as by observations.[15,16] It is important to realize that the drift waves (DW) and zonal flows (ZFs) form a self-regulating system so that each cannot be addressed in isolation. Namely, zonal flow energy is fed by the drift waves, and thus reduces their intensity. Conversely, the viability of ZFs is a key to DW turbulence and transport reduction. Rosenbluth and Hinton have recently shown[17,18] that the linear, time-asymptotic damping of ZFs in toroidal devices is due to collisional friction, only. Therefore, collisions must be crucial to the regulation of transport. In particular, the ZF saturation mechanism, central to this self-regulation, is strongly influenced by ion-ion collisions.[19] Since zonal flows reduce transport and turbulence, and collisions damp flows, it follows that ion friction must ultimately control transport. Such a causal relationship has been confirmed in recent numerical simulations.[19]

The question of what happens at zero collisionality motivates the consideration of a second class of phenomena, related to the so-called ''Dimits shift,'' that has been observed in Ref. 12. This regime consists of a strong suppression of the DW turbulence and transport at a nonzero growth rate of the ITG instability near the marginal stability point. It has been identified with a residual ZF that, being essentially undamped, shears the DWs down to vanishingly small amplitudes. Large DW amplitude is not necessary to drive the flow since the flows are (essentially) undamped. Thus, the Dimits shift regime constitutes a rather atypical corner of parameter space. The ZF saturation mechanism is not completely understood in this case but is most probably nonlinear,[19] and the destruction of the ZF by Kelvin–

[a]Electronic mail: mmalkovphysics.ucsd.edu

Helmholtz like instability is a potentially interesting candidate for ZF saturation mechanism.[20] Accordingly, in the Dimits shift regime the ZF generation should be addressed differently than it is treated in the case of finite collisionality, i.e., as in Refs. 21,22, and further in this paper. Namely, the approximation of vanishingly small DW amplitude should be invoked. We devoted separate publications to generation of ZFs by DWs in this case[23,24] where the DW amplitude threshold for the flow amplification instability is calculated for arbitrary DW spectra. In the present paper, the critical question of how the drift wave–zonal flow system saturates will be addressed from the perspective of self-regulation by feedback of the zonal flows on the DW spectrum.

Turning to the methodology of the DW–ZF self-regulation, we note that many approaches have been based on low-dimensional, Galerkin-type models.[6,25–27] Indeed, a broad spectrum of ZF modes typically exists, both in gyrokinetic simulations[9] and in planetary atmospheres.[28] These works generally require the presence of a strong damping at small scales, naturally given by the viscosity and thermal conductivity in the hydrodynamic cases. As we mentioned, however, zonal flows in toroidal devices are damped only by collisions and may thus develop quite complicated radial structures that cannot be described by models with only a small number of modes. Moreover, the spectrum of the DWs, being sheared by the ZF, is substantially broader in comparison to that one would expect from linear instability, due to high k_r generation, as observed in gyrokinetic simulations.[14] This necessitates a theory capable of describing DW and ZF spectra as coupled elements of the corpus of self-organized turbulence, without lumping their description into a few spectral components. Recently, such a spectral level model for zonal flow problem has been suggested in Ref. 21. In short, that work produced two coupled evolution equations of the ''predator–prey'' type. One of them is an equation for the ZF amplitude (''predator'') driven by the modulationally unstable drift waves. The second one is for the number of the DW quanta (''prey'') that suffer random shearing in the ZF field. This is described by the diffusion term in the radial wave number k_r. The randomness of the shearing emphasizes the necessity of an infinitely dimensional (non-Galerkin) treatment, since it results in chaotic dynamics of the rays of drift waves.[22] Ray chaos is the key to irreversibility of the DW spectral evolution and ultimately is what allows the use of quasilinear theory. The spectral ''predator–prey'' approach, while having an advantage over the low-dimensional models due to the *spectral* description of the turbulence, represents, at the same time, a significant reduction of the initial fully nonlinear PDE system because it identifies critical turbulence components and is, in essence, quasilinear in structure.

The ray chaos of drift waves in zonal flows not only requires new approaches to the saturation mechanisms but also has a significant impact on the particle transport. As it was demonstrated in Ref. 22, along with the familiar wave decorrelation caused by the Doppler shift in a sheared mean flow, the random shear in the zonal flows represents an additional stochastic variable over which the particle excursion should be averaged in order to calculate their transport. The required ergodic property of the ZF field with respect to the transport driving drift waves is ensured by the overlap of individual group resonances $\Omega/q \simeq V_{\mathrm{gr}}$ between the radial ZF phase and DW group velocities. Here, Ω must be interpreted as being nonlinearly broadened. The required high density of the distribution of the ZFs in phase velocity Ω/q is, in turn, a result of their low frequency (linearly, ZF is a zero frequency mode) and spatial complexity (broad q-spectrum).[22]

In the present paper we quantitatively study the stationary spectra of coupled DW–ZF turbulence from the perspective of the ''predator–prey'' model. The focus is on the scaling of the turbulence and transport levels with the ZF collisional damping, γ_d and on morphology of the turbulence spectra.

Depending on the relation between the time scales of ZF damping and DW generation γ_d/γ, two distinct regimes occur. If this ratio is small, the DWs are very efficiently sheared by ZFs (i.e., via nonlocal interaction in **k**-space) so that their amplitude scales linearly with γ_d. If γ_d/γ is large, the DWs saturate via local interaction and the turbulence level will be independent of γ_d. Of course, determining the value of γ_d/γ at crossover is especially critical to predictions of transport scaling.

An interesting finding of this investigations is that *multiple saturated states are possible*. Starting from a critical ZF damping rate $\gamma_d = \gamma_{dc}$, two new solutions, with considerably higher DW intensity levels, branch off from the expected one. Of the three solutions, the intermediate one is unstable. The solution with smaller turbulence intensity (which saturates via γ_d) is characterized by strong shearing of DWs. The higher intensity one, based on its spectral properties (condensate in k_r), consists of radially elongated features in the DW turbulence which may be tentatively identified with radial cells (e.g., Ref. 29). We refer to this solution as the condensate. Cyclic bifurcation transitions between these two states are possible, as well.

By studying these solutions we address the following issues.

(1) The saturation mechanism and scalings of the drift wave turbulence away from the threshold of linear stability.
(2) The transition region from linear scaling of drift wave intensity with γ_d to a saturation regime independent of γ_d.
(3) The forms of the stationary DW and ZF spectra.
(4) The stability of stationary solutions.

The remainder of this paper is organized as follows. In Sec. II we introduce the basic model and equations. Section III deals with determining the drift wave spectra in a given zonal flow field. In Sec. IV we address the back reaction of the drift waves on the zonal flow and calculate both spectra, self-consistently. After an analysis of the results in Sec. V, we conclude in Sec. VI with a summary and discussion of future work.

II. BASIC MODEL

In this section we introduce an evolution equation that governs the dynamics of drift waves in the straining field of

zonal flows. As a next step, we obtain an equation for the zonal flow which essentially arises from the modulational instability of the drift wave packets. We will closely follow Ref. 21 paying, however, more attention to some details of the derivation.

A. Drift wave evolution

We start from the wave kinetic equation for the number of quanta of the drift waves $N_{\mathbf{k}}$ propagating in the presence of a zonal velocity field. The DWs are subject to a linear instability (e.g., ITG instability) and nonlinear self-interaction. These are given on the right-hand side (rhs) of Eq. (1) below. The propagation part of this equation [left-hand side (lhs)] in configuration $\mathbf{x}=(r,\theta)$ and wavevector $\mathbf{k}=(k_r,k_\theta)$ space may be described within the eikonal approach. It allows the *ansatz* of conservation of $N_{\mathbf{k}}$ along the wave rays when the rhs is absent. The waves propagate, as usual, along the lines of constant frequency of the drift waves, Doppler shifted by the local zonal flow velocity. The equation thus reads

$$\frac{dN_{\mathbf{k}}}{dt}\equiv\frac{\partial N_{\mathbf{k}}}{\partial t}+(\mathbf{V}_g+\mathbf{V}_E)\cdot\frac{\partial N_{\mathbf{k}}}{\partial\mathbf{x}}-k_\theta\frac{\partial V_E}{\partial\mathbf{x}}\cdot\frac{\partial N}{\partial\mathbf{k}}$$
$$=\gamma_{\mathbf{k}}N_{\mathbf{k}}-St\{N_{\mathbf{k}}\}. \tag{1}$$

Here $\mathbf{V}_E$ is the zonal flow velocity assumed to be in θ-direction, $\mathbf{V}_E=\hat{\theta}V_E$. $St\{N_{\mathbf{k}}\}$ is a nonliner collision integral which captures local nonadiabatic (i.e., local in k-space) mode–mode interactions. Adiabatic, nonlocal interactions are accounted for by the refraction term in Eq. (1). First, we simplify the rhs of this equation by making an assumption that during the evolution of the drift wave spectrum, not only the usual eikonal requirements are met ($dN_{\mathbf{k}}/dt<N_{\mathbf{k}}\omega_{\mathbf{k}}$, i.e., $qV_{\rm gr}<\omega_{\mathbf{k}}$, where q is the radial wave number of the ZF and DW packet purturbarion) but also the terms on the rhs must remain approximately in balance, i.e., $dN_{\mathbf{k}}/dt\ll\gamma_{\mathbf{k}}N_{\mathbf{k}}$. Then, a natural way to proceed is to make the *ansatz*

$$N_{\mathbf{k}}=N_B+N^{(1)}, \tag{2}$$

where N_B is an equilibrium that null the rhs of Eq. (1):

$$\gamma_{\mathbf{k}}N_B-St\{N_B\}=0. \tag{3}$$

The problem of determining the stationary turbulence spectra [i.e., solving Eq. (3)] is a problem in its own right. Clearly, its solution depends on the particular form of the drift wave "collision" term $St(N_{\mathbf{k}})$ (see, e.g., Ref. 4 and references therein). Its solution N_B, in the context of Eq. (1), would be still underdetermined and contain an arbitrary dependence on time. The next standard step would be to expand the nonlinear functional on the rhs of Eq. (1) for small $N^{(1)}$ and to submit N_B to the (small) lhs. Note that if the St-term is quadratic, this linearization together with the balance (3) will effectively flip the sign in the linear part of the lhs of Eq. (1) turning the linear instability $\gamma_{\mathbf{k}}$ into damping $-\gamma_{\mathbf{k}}$ with the corresponding modification of the linear DW packet propagator $(\Omega-qV_{\rm gr})^{-1}$ [see Ref. 21 and Eq. (9) below]. The solubility condition for $N^{(1)}$ should yield an evolution equation for N_B. This asymptotic scheme is proven very efficient for cases in which the DW interaction may be regarded as "static," in the sense that its form remains unchanged during the evolution of N caused by the adiabatic interaction with zonal flows [reflected on the lhs of Eq. (1)]. If, however, this interaction is expected to be strong, it should also influence the way the drift waves interact with each other on a much longer time scale. Under these circumstances we seek to apply a somewhat different ordering. First, we split the perturbed part $N^{(1)}$ along with V_E as follows:

$$N_{\mathbf{k}}=N_B+N_{\mathbf{k}}^{(1)}=N_B+\langle N(k_r,t)\rangle+\tilde{N}_{\mathbf{k}}, \tag{4}$$

$$V_E=\langle V_E\rangle+\tilde{V}_E. \tag{5}$$

The averaging operation $\langle\ \rangle$ will be performed over the short spatial scales. The difference between the two "background" wave densities N_B and $\langle N\rangle$ is in the action of the wave propagation operator on the lhs of Eq. (1) on them. Namely, it is assumed that the N_B varies very slowly in time and in both configuration and $\mathbf{k}$-space so that $dN_B/dt\simeq 0$, while the $\langle N\rangle$ evolves in time and k_r. To obtain an equation for $\langle N\rangle$, it is convenient to rewrite Eq. (1) in conservative form

$$\frac{\partial}{\partial t}N_{\mathbf{k}}^{(1)}+\frac{\partial}{\partial\mathbf{k}}\cdot\left[(\omega+\mathbf{k}\cdot\mathbf{V}_E)\frac{\partial}{\partial\mathbf{x}}N_{\mathbf{k}}^{(1)}\right]$$
$$-\frac{\partial}{\partial\mathbf{x}}\cdot\left[(\omega+\mathbf{k}\cdot\mathbf{V}_E)\frac{\partial}{\partial\mathbf{k}}N_{\mathbf{k}}^{(1)}\right]=\gamma_{\mathbf{k}}N_{\mathbf{k}}-St\{N_{\mathbf{k}}\}. \tag{6}$$

Here the drift wave frequency is $\omega_{\mathbf{k}}=k_\theta V_*(1+k_\perp^2\rho_s^2)^{-1}$ where the drift velocity $V_*=-(cT_e/eB)d\ln n_0/dr$. As stated, we neglect the slow variation of N_B on the lhs. Furthermore, we simplify the rhs by expanding it around N_B

$$\gamma_{\mathbf{k}}N_{\mathbf{k}}-St\{N_{\mathbf{k}}\}\simeq\gamma_{\mathbf{k}}N_{\mathbf{k}}^{(1)}-\frac{\Delta\omega_{\mathbf{k}}}{N_B}(N_{\mathbf{k}}^{(1)})^2. \tag{7}$$

We have taken the quadratic part of expansion of the functional $St\{\cdot\}$ in the simplest, algebraic form. The linear in $N_{\mathbf{k}}^{(1)}$ part of the St-term (if present) can be included in the $\gamma_{\mathbf{k}}$-term. Neglecting the $\tilde{N}^2$ contribution to the rhs of Eq. (7), after simple manipulations on Eq. (6), we obtain for $\langle N\rangle$ the following equation:

$$\frac{\partial}{\partial t}\langle N\rangle+\frac{\partial}{\partial k_r}\Gamma_{\mathbf{k}}=\gamma_{\mathbf{k}}\langle N\rangle-\frac{\Delta\omega_{\mathbf{k}}}{N_B}\langle N\rangle^2, \tag{8}$$

where the flux in k_r is given by

$$\Gamma_{\mathbf{k}}=-k_\theta\left\langle\tilde{N}_{\mathbf{k}}\frac{\partial\tilde{V}_E}{\partial r}\right\rangle$$

(we assume for simplicity that $\langle V_E\rangle=0$). Both $\tilde{N}_{\mathbf{k}}$ and $\tilde{V}_E$ are assumed here to vary slowly in r as compared to the typical k_r involved. We may thus relate them by making another *ansatz*, $\tilde{V}_E(r,t)\sim\tilde{V}_q e^{-i\Omega_q t+iqr}$, $\tilde{N}_{\mathbf{k}}(r,t)\sim\tilde{N}_{\mathbf{k},q}e^{-i\Omega_q t+iqr}$. Substituting Eqs. (4) and (5) into Eq. (1) after linearization we obtain

$$\tilde{N}_q=-\frac{qk_\theta\tilde{V}_q}{\Omega_q-qV_{\rm gr}+i\gamma_{\mathbf{k}}}\frac{\partial}{\partial k_r}\langle N\rangle. \tag{9}$$

We have used the approximate balance condition

$$\gamma_{\mathbf{k}} \simeq (\Delta\omega/N_B)\langle N\rangle \tag{10}$$

to simplify the linearized rhs of Eq. (1). Equation (8) then takes the following final form:[21]

$$\frac{\partial\langle N\rangle}{\partial t} - \frac{\partial}{\partial k_r} D_{\mathbf{k}} \frac{\partial\langle N\rangle}{\partial k_r} = \gamma_{\mathbf{k}}\langle N\rangle - \frac{\Delta\omega_{\mathbf{k}}}{N_B}\langle N\rangle^2, \tag{11}$$

where the $k_r k_r$ component of the drift wave diffusion tensor is given by

$$D_{\mathbf{k}} = \sum_q k_\theta^2 q^4 \rho_s^2 c_s^2 \left(1 - \frac{q^2\rho^2}{1+k_\perp^2\rho_s^2}\right)^2 R(\mathbf{k},q)|\hat{\Phi}_q|^2. \tag{12}$$

Here the second term in parentheses (<1) comes from the density modulation. The dimensionless potential and velocity of zonal flow are related by $\tilde{V}_q = iq(cT_e/eB)\hat{\Phi}_q$ and the particle response function to the perturbation is given by the following expression:

$$R(\mathbf{k},q) = \frac{\gamma_{\mathbf{k}}}{q^2 V_{\mathrm{gr}}^2 + \gamma_{\mathbf{k}}^2} \tag{13}$$

in which we neglected Ω compared to qV_{gr}. Note that this form of the DW propagator in the ZF field explicitly emphasizes their linear instability growth rate $\gamma_{\mathbf{k}}$ as a surrogate for the nonlinear resonance broadening $\Delta\omega$, in view of its relation to the nonlinear St-term in Eq. (6) through the balance condition Eq. (10).

B. Zonal flow evolution

A straightforward way to describe zonal flows is to utilize a simple fluid model (see, e.g., Ref. 30). The electron transport is governed by

$$\frac{dn}{dt} + \nabla_\parallel (n v_\parallel) = 0, \tag{14}$$

where

$$\frac{d}{dt} \equiv \frac{\partial}{\partial t} + \mathbf{V}_E\nabla,\ \mathbf{V}_E = \frac{c}{B}\mathbf{e}_\parallel \times \nabla\phi$$

and ϕ is the total electrostatic potential (zonal flow plus drift waves). In the ion continuity equation, the polarization drift should be retained along with the common **E×B** drift instead of the longitudinal transport in the above equation for electrons. Thus, the ion transport is governed by

$$\frac{dn}{dt} - \frac{Mc^2}{eB^2}\nabla_\perp \cdot \left(n\frac{d}{dt}\nabla_\perp\phi\right) = 0, \tag{15}$$

where the quasineutrality requirement $n_e = n_i \equiv n$ has been used. Now we split the total density and potential perturbations as

$$n = N + \tilde{n} + n_0(r),\ \phi = \Phi + \tilde{\phi}, \tag{16}$$

where N and Φ stand for poloidally and toroidally symmetric zonal flow type perturbations, so that from Eq. (14) we have $dN/dt = 0$. For the drift wave type perturbations we have simply an adiabatic response $\tilde{n}/n_0 = e\tilde{\phi}/T_e$. Having this in mind from (15), one obtains[30,31]

$$\left(\frac{\partial}{\partial t} + V_0\frac{\partial}{\partial\theta}\right)\tilde{\phi} + V_*\frac{\partial\tilde{\phi}}{\partial\theta} - \rho_s^2\left(\frac{\partial}{\partial t} + \mathbf{V}_E\nabla\right)\nabla_\perp^2\phi = 0, \tag{17}$$

where V_0 is the zonal flow part of the **E×B** drift, $V_0 = (c/B)\partial\Phi/\partial r$ and $V_* = -(cT_e/eB)d\ln n_0/dr$. Averaging the last equation over poloidal and toroidal directions, which is also denoted here by $\langle\cdot\rangle$ (not to be confused with notations of Sec. II A), taking into account $\langle\tilde{\phi}\rangle = 0$ and, ignoring the mean radial gradient $\nabla\Phi_0$, one obtains the following equation for zonal flow generation

$$\frac{\partial\Phi}{\partial t} + \frac{\gamma_d}{2}\Phi = \frac{c}{B}\left\langle\frac{\partial\tilde{\phi}}{\partial r}\frac{\partial\tilde{\phi}}{\partial\theta}\right\rangle. \tag{18}$$

We have added the collisional damping γ_d in a standard way.[17] Making the *ansatz* $\Phi \sim \Phi_q \exp(+iqr)$ and assuming that $q \ll \Delta k_r$, where Δk_r denotes the width of the drift wave spectrum in k_r, the last equation is transformed to

$$\left(\frac{\partial}{\partial t} + \frac{1}{2}\gamma_d\right)\Phi_q = \frac{c}{B}\sum_{\mathbf{k}_1+\mathbf{k}_2=\mathbf{q}} k_{1r}k_{2\theta}\tilde{\phi}_{\mathbf{k}_1}\tilde{\phi}_{\mathbf{k}_2}. \tag{19}$$

As in the preceding section, the perturbation to the drift wave spectrum caused by the emerging zonal flows may be described by the eikonal equation (6) in which the density of the drift wave quanta is related to $|\tilde{\phi}_{\mathbf{k}}|^2$ through $N_{\mathbf{k}}^{(1)} = (1+k_\perp^2\rho_s^2)|e\tilde{\phi}_{\mathbf{k}}/T_e|^2/\omega_{\mathbf{k}}$. Again, we assume that the drift wave spectrum consists of an equilibrium part $\langle N\rangle$ and a perturbed part $\tilde{N}_{\mathbf{k}} = N_{\mathbf{k}}^{(1)} - \langle N\rangle$. Substituting $\tilde{N}_{\mathbf{k}}$ from Eq. (9) into Eq. (19) and using also Eq. (17) one obtains the following equation for the dimensionless zonal flow potential $\hat{\Phi}_q = e\Phi_q/T_e$ (Ref. 21):

$$\begin{aligned}(\partial_t + \gamma_d)|\hat{\Phi}_q|^2 &= -q^2c_s^2\sum_{\mathbf{k}}\frac{k_\theta^2\rho_s^2\omega_{\mathbf{k}}k_r}{1+k_\perp^2\rho_s^2}\frac{\partial\langle N\rangle}{\partial k_r}R(\mathbf{k},q)|\hat{\Phi}_q|^2 \\ &+ \frac{4\Omega_i^2c_s^2}{L_n^2}\sum_{\mathbf{k}} k_r^2\rho_s^2(k_\theta^2\rho_s^2)^2\frac{\langle N\rangle^2}{(1+k_\perp^2\rho_s^2)^4}R(\mathbf{k},q).\end{aligned} \tag{20}$$

Here the first term on the rhs is due to the modulational instability of the drift wave turbulence. The second term corresponds to the noise emitted into the zonal flow by the incoherent drift wave coupling to a perturbation with $q_\theta = 0$ and finite q_r. This particular form of the noise is calculated using two-dimensional hydrodynamics and is necessarily of second order in Reynolds stress.

III. DRIFT WAVE DYNAMICS IN THE ZONAL FLOW SHEAR

In this section we analyze the drift wave dynamics in a prescribed zonal flow spectrum. This approach appears to be efficient because the drift wave diffusion coefficient $D_{\mathbf{k}}$ [Eq. (12)] depends on the zonal flow spectrum and thus on the drift wave spectrum $\langle N\rangle$ itself only as a functional, i.e., in

practice, it contains just one or a few parameters determining $\langle N\rangle$, most notably its amplitude. This will be calculated in the next section, after the general form of the solution $\langle N(\mathbf{k})\rangle$ is obtained. To begin, we treat $D_{\mathbf{k}}$ as a given function with a reasonable behavior.

The dynamics of the drift waves, as Eq. (11) suggests, may fall into two different regimes. One is a quasilinear regime in which the nonlinear term in Eq. (11) is small everywhere and one may expect a steady state in which drift waves generated in the region where $\gamma(k_r)>0$ are diffusively spread in k_r over the region where $\gamma(k_r)<0$ and linearly damped therein. Even in the case of strong nonlinear coupling, the DW spectrum should decay asymptotically for sufficiently large k_r, where $\gamma<0$ so that the nonlinear term becomes negligible. However, within and not far away from the region where $\gamma>0$, the amplitude of the drift waves may be high, so that they can be nonlinearly damped without significant cascade to short scales. This is a second, strongly nonlinear or ''mixing length'' type regime. We start from the first one and consider a more general case, which also includes the second regime, later in Sec. III B.

A. Quasilinear regime of drift wave interaction with the zonal flow

Looking for a steady state solution of Eq. (11) and neglecting the nonlinear term, we may write

$$-\frac{\partial}{\partial k_r}D_{\mathbf{k}}\frac{\partial\langle N\rangle}{\partial k_r}=\gamma_{\mathbf{k}}\langle N\rangle. \tag{21}$$

We assume that $\gamma(k_r)\geqslant 0$ for $|k_r|\leqslant k_0$ and is negative otherwise. Introducing a new variable

$$\xi=\int_0^{k_r}\frac{dk_r}{D(k_r)}$$

Eq. (21) can be rewritten as

$$\frac{d^2}{d\xi^2}\langle N\rangle-Q(\xi)\langle N\rangle=0, \tag{22}$$

where $Q=-\gamma D$. The physically relevant solution must have the following asymptotic behavior at $\xi\to\pm\infty$

$$\langle N\rangle\sim\frac{1}{Q^{1/4}}\exp\left(\mp\int_{\pm\xi_0}^{\xi}\sqrt{Q}\,d\xi\right), \tag{23}$$

where $\xi_0=\xi(k_0)$. For this to be true, Q must satisfy one of the following relations (quantization rule)

$$\int_{-\xi_0}^{\xi_0}\sqrt{-Q}\,d\xi=\pi(n+\tfrac{1}{2}) \tag{24}$$

with integral $n\geqslant 0$. Formally, the WKB result used here is asymptotically correct only for $n\gg 1$, whereas we are interested in the opposite case, namely $n=0$ ($\langle N\rangle$ should not have zeroes on the real ξ-axis). At the same time it is known (see, e.g., Ref. 32) that result of Eq. (24) is a good approximation for smooth potentials Q also in the case $n=0$. For example, when Q is a quadratic function [indeed, in the case of smooth coefficients $\gamma_{\mathbf{k}}$ and $D_{\mathbf{k}}$ it can be replaced by its quadratic expansion in Eq. (24) for precisely the case of small n], the result (24) is exact for all $n\geqslant 0$. Returning to the variable k_r, from (24) we thus obtain

$$\int_{-k_0}^{k_0}\sqrt{\frac{\gamma}{D}}dk_r=\frac{\pi}{2}. \tag{25}$$

This relation fixes the normalization of $\langle N\rangle$ (the stationary level of drift wave turbulence) in the quasilinear regime, since D depends on it through the amplitude of zonal flows, Eqs. (12) and (20). We shall determine it after the nonlinear case is considered in the next section.

B. Simplified nonlinear model of DW–ZF coupling

The above treatment of the quasilinear case suggests that the interaction of the drift waves with the self-generated zonal flows may be understood in the frame of a simplified model that takes into account the following key ingredients of this process: (i) there are two physically distinct regions in ω-space; the first region is that of excitation of drift waves by a linear instability and the second is where they are linearly and nonlinearly damped via shearing to high k_r, (ii) zonal flows generated by the drift waves drive a diffusive flux of the drift waves from the first region to the second one via random refraction. The intensity of zonal flows, drift waves, and associated thermal transport are essentially determined from their mutual adjustment in a self-regulating manner, (iii) since zonal flows are poloidally directed, the flux of the drift waves in $\mathbf{k}$-space is directed along k_r.

Based on the above considerations we simplify the main system of equations derived in the preceding sections as follows. Because of (iii) we do not consider the k_θ structure of the spectrum and average Eq. (11) over k_θ. Effectively, we replace k_θ by $\overline{k_\theta}$ which, strictly speaking, remains unknown but can be estimated from the maximum of $\gamma(\mathbf{k})$. Next, we simplify the diffusive transport of the drift waves and replace $D(k_r)$ by its averaged value $\overline{D}$ in Eq. (11). Note that $\overline{D}$ is still a functional of $\langle N\rangle$, which is more important here than the k_r dependence of D. Finally, since we focus on the simple scenario outlined by (i) and (ii) rather than on the details of the excitation and damping of the spectrum, we represent $\gamma(k_r)$ as a step function

$$\gamma(k_r)=\begin{cases}\gamma^+, & |k_r|\leqslant k_{0,}\\ -\gamma^-, & |k_r|>k_0.\end{cases} \tag{26}$$

Here k_0 is the k_θ-averaged position of the neutral curve in the k_θ,k_r plane and $\gamma^\pm$ are positive constants. Equation (11) is thus

$$\frac{\partial\langle N\rangle}{\partial t}-\overline{D}\frac{\partial^2\langle N\rangle}{\partial k_r^2}=\gamma\langle N\rangle-\frac{\Delta\omega}{N_B}\langle N\rangle^2. \tag{27}$$

Assuming stationarity we arrive at the following dynamical system, in which the independent variable k_r may be regarded as ''time:''

$$\overline{D}\frac{d^2\langle N\rangle}{dk_r^2}+\gamma(k_r)\langle N\rangle-\frac{\Delta\omega}{N_B}\langle N\rangle^2=0. \tag{28}$$

We may now easily find a formal solution of the last equation assuming for simplicity that the coefficient $\Delta\omega/N_B$ does not depend on k_r. Since $\langle N\rangle$ and thus $d\langle N\rangle/dk_r$ must be continuous at $k_r=k_0$, the first integral of Eq. (28) can be written as follows:

$$\frac{d\langle N\rangle}{dk_r}=-\frac{1}{\sqrt{\overline{D}}}\begin{cases}\sqrt{(\gamma^+ +\gamma^-)N_0^2-\gamma^+\langle N\rangle^2+(2\Delta\omega/3N_B)\langle N\rangle^3}, & k_r\leqslant k_0;\\ \langle N\rangle\sqrt{\gamma^- +(2\Delta\omega/3N_B)\langle N\rangle}, & k_r>k_0.\end{cases} \tag{29}$$

We have used obvious requirements of vanishing of $\langle N\rangle$ and $d\langle N\rangle/dk_r$ at $k_r=\infty$ and denoted by $\langle N(k_0)\rangle=N_0$. On the negative half-axis $k_r<0$, the spectrum can be recovered from the symmetry requirement $\langle N(-k_r)\rangle=\langle N(k_r)\rangle$. The solution for $k_r>k_0$ is trivially found to be

$$\langle N\rangle=\frac{3N_B\gamma^-}{2\Delta\omega}\sinh^{-2}\left[\frac{1}{2}(\gamma^-/\overline{D})^{1/2}(k_r-k_1)\right], \tag{30}$$

where the integration constant k_1 is determined by the condition $\langle N(k_0)\rangle=N_0$. The quantity N_0 can be conveniently used for the classification of different solutions. While they all have similar behavior at $|k_r|>k_0$, in the long wave region $k_r\leqslant k_0$ we will distinguish between spectra that are regular and singular (condensate type solutions) at $k_r=0$. Clearly, in the latter case a cutoff at some $k_r=k_{\min}\ll k_0$ (which, in fact, always exists due to the finite radius of the system) needs to be introduced. These two classes of solutions are seen on the phase plane of Eq. (29) shown in Fig. 1. The condition $|k_r|=k_0$ taken at different N_0 forms a special manifold on the $(\langle N\rangle, d\langle N\rangle/dk_r)$ plane, which is determined by the lower equation (29), and consists of two branches crossing at the origin (note that this manifold does not depend on the parameter N_0) so that all orbits of Eq. (29) belong to this manifold for all $|k_r|>k_0$. Turning to the region $|k_r|\leqslant k_0$, we observe that for sufficiently small $N_0\equiv\langle N(k_0)\rangle$, there is a family of regular solutions (homoclinic orbits) that leave the special manifold at $k_r=k_0, \langle N\rangle=N_0$, and return to it at $k_r=-k_0, \langle N\rangle=N_0$, thus making a closed loop with $d\langle N\rangle/dk_r=0$ at $k_r=0$ (Fig. 1). These solutions require satisfying the following condition:

$$N_0<(\gamma^+/\Delta\omega)3^{-1/2}(1+\gamma^-/\gamma^+)^{-1}\equiv N_{cr} \tag{31}$$

that ensures the existence of two real roots at $\langle N\rangle>N_0$ of the polynomial under square root in the upper Eq. (29). For $N_0>N_{cr}$, the solutions diverge at $k_r=0$ as $\langle N\rangle\sim 1/k_r^2$. The separatrix solution corresponds to a spectrum that approaches the "box" function $\gamma(k_r)$ in the region $|k_r|\leqslant k_0$, Fig. 2. We consider both type of solutions separately in the following two sections. We write the solution of Eq. (29) in the region $k_r\leqslant k_0$ in the implicit form

$$\frac{k_0-k_r}{\sqrt{\overline{D}}}=\int_{N_0}^{\langle N\rangle}\frac{dN}{\sqrt{(\gamma^+ +\gamma^-)N_0^2-\gamma^+N^2+(2\Delta\omega/3N_B)N^3}}. \tag{32}$$

The solution $\langle N(k_r)\rangle$ may be obtained in terms of elliptic functions. According to the above qualitative analysis, if $N_0\leqslant N_{cr}$, there is a family of regular solutions $\langle N(k_r)\rangle$ that are finite for all k_r. In this case, the upper limit of the integral in the lhs is a root of the polynomial in the integrand. For $N_0>N_{cr}$, the solutions are singular, which means that the integral on the rhs *converges* as $\langle N\rangle\to\infty$. The phase plane of Eq. (28) with both types of the drift wave spectra as well as a separatrix solution is shown in Fig. 1. The classification of these solutions is based on the number of real

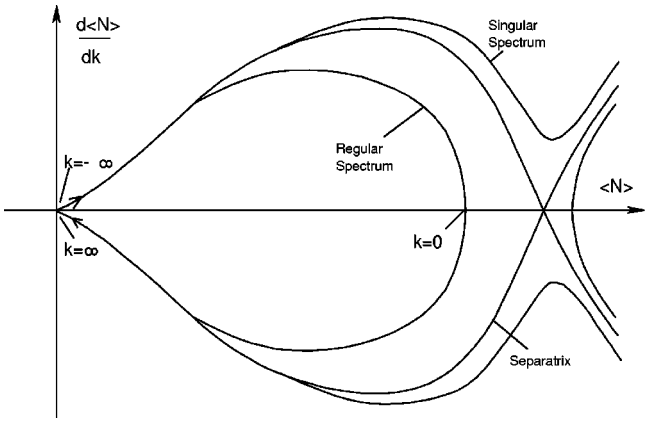

FIG. 1. Phase plane of Eq. (29).

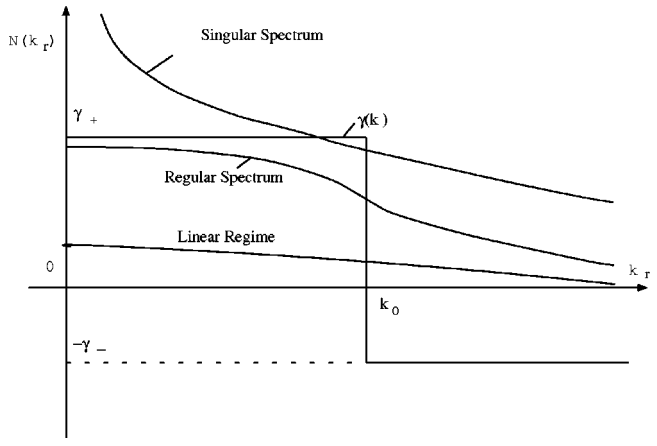

FIG. 2. Solutions for $\langle N(k_r)\rangle$ corresponding to the phase curves shown in Fig. 1.

roots of the cubic polynomial on the rhs of Eq. (32), which is equal to either three or one. We start from the former possibility.

1. Regular spectrum

In the case of the regular spectrum, the polynomial in Eq. (32) has three real roots, so that the integral must be taken between N_0 and the middle root of the polynomial at $\langle N\rangle = N_1 < \infty$, while k_r should be set to $k_r = 0$ by the symmetry of the spectrum [i.e., $N_1 = \langle N(k_r=0)\rangle$ see Fig. 1]. It is convenient to normalize the spectral amplitude to the mixing length scaling, namely to introduce the following dimensionless quanta density:

$$\mathcal{N} = \frac{\Delta\omega}{\gamma^+}\frac{\langle N\rangle}{N_B}. \tag{33}$$

For the sake of convenience, we perform the integration in Eq. (41) using a shifted variable $z = \mathcal{N} - 1/2$. Setting $k_r = 0$, Eq. (32) can be rewritten as

$$\frac{k_0\sqrt{\gamma^+}}{\sqrt{\bar{D}}} = \sqrt{\frac{3}{2}}\int_b^{z_0}\frac{dz}{\sqrt{z^3 - 3z/4 + a/4}}. \tag{34}$$

Here

$$a = 6\frac{\mathcal{N}_0^2}{\alpha} - 1, \quad b = \mathcal{N}_0 - \frac{1}{2}, \quad \mathcal{N}_0 = \frac{\Delta\omega}{\gamma^+}\frac{N_0}{N_B},$$
$$\alpha = \gamma^+/(\gamma^+ + \gamma^-) \tag{35}$$

and z_n are the three roots of the polynomial in Eq. (34)

$$z_n = \sin\left[\tfrac{1}{3}\arcsin(a) + \tfrac{2}{3}\pi n\right], \quad n = -1, 0, 1. \tag{36}$$

For the case of regular spectrum considered here [i.e., as in Eq. (31)], $a < 1$. Evaluating the integral in Eq. (34) we obtain

$$\frac{k_0\sqrt{\gamma^+}}{\sqrt{\bar{D}}} = 2(1-\kappa^2+\kappa^4)^{1/4}\left[\mathbf{K}(\kappa) - F(\sin^{-1}\sqrt{u}, \kappa)\right]$$
$$\equiv J_r(\mathcal{N}_1), \tag{37}$$

where we have introduced the following notation:

$$u = \frac{\sqrt{\alpha}\sqrt{1 - 2\mathcal{N}_1/3} + \sqrt{\alpha}\sqrt{2\mathcal{N}_1 + 1} + 2}{3 + \sqrt{(2\mathcal{N}_1+1)/(1-2\mathcal{N}_1/3)}}, \tag{38}$$

F and $\mathbf{K}$ are the incomplete and complete elliptic integrals of the first kind, respectively. Note that their modulo κ depends only on $\mathcal{N}_1 \equiv (\Delta\omega/\gamma^+)N_1/N_B$ and is given by

$$\kappa = \frac{1}{\sqrt{2}}\sqrt{1 + \frac{2\mathcal{N}_1 - 1}{\sqrt{(1+2\mathcal{N}_1)(1-2\mathcal{N}_1/3)}}}. \tag{39}$$

It is important to emphasize that Eq. (37) is in fact an equation for the normalized DW amplitude $\mathcal{N}_1$ (or equivalently, for $\mathcal{N}_0$) since the DW diffusivity $\bar{D}$ depends on $\mathcal{N}_1$ via Eq. (20). The quantity $\mathcal{N}_0$ is related to $\mathcal{N}_1$ through [see Eqs. (35) and (36)]

$$\mathcal{N}_1 = \frac{1}{2} + \sin\left[\frac{1}{3}\arcsin\left(6\frac{\mathcal{N}_0^2}{\alpha} - 1\right)\right]. \tag{40}$$

Recall that $\mathcal{N}_1 \leqslant 1$ and $\mathcal{N}_0 \leqslant \sqrt{\alpha/3}$. For larger $\mathcal{N}_0$, the spectrum becomes singular at $k_r = 0$.

2. Singular spectrum

The formation of the regular spectrum, considered above, is a consequence of the balance between the instability term in Eq. (27) on the one hand, and the remaining two terms that describe the refraction in k_r and the local nonlinear coupling on the other. Clearly, the nonlinear term always stabilizes the spectrum while the refraction can locally destabilize it where $\langle N\rangle$ is concave. This is the case for the singular spectrum. One sees that a spectrum that behaves as $\langle N\rangle \propto 1/k_r^2$ may form at small k_r by the balance between the refraction and nonlinearity (both were the stabilizing terms for the regular spectrum) in which the instability term is unimportant. *Thus, the condensate solution is a consequence of the interplay between local and nonlocal nonlinear interaction*. Here we obtain an *exact* solution for such a spectrum in the frame of our simple instability model already used in the preceding section.

In the case of singular spectrum the polynomial on the rhs of Eq. (32) has only one real root, so that $\langle N\rangle$ becomes infinite at $k_r = 0$. In this case the spectrum must be cut off at some small $k_r = k_{\min}$, that is clearly limited by at least $2\pi/a$ where a is the minor radius or, perhaps more realistically, by the characteristic scale of the driving profile. Equation (32) then takes the form

$$\frac{k_0 - k_{\min}}{\sqrt{\bar{D}}} = \int_{N_0}^{N_{\max}}\frac{dN}{\sqrt{(\gamma^+ + \gamma^-)N_0^2 - \gamma^+ N^2 + (2\Delta\omega/3N_B)N^3}}. \tag{41}$$

For the solution not too close to the separatrix (see Fig. 1) and assuming $k_{\min} \ll k_0$ we can set $N_{\max} = \infty$ and $k_{\min} = 0$ here. Evaluating the integral we obtain the following counterpart of Eq. (37) for the case of the singular spectrum:

$$\frac{k_0\sqrt{\gamma^+}}{\sqrt{\bar{D}}} = \left(\frac{3}{4q^2-1}\right)^{1/4} F(\phi, \kappa) \equiv J_s(\mathcal{N}_0). \tag{42}$$

Here we have used the notation

$$\cos\phi = \frac{\sqrt{3}\sqrt{4q^2-1} + 1 - 2q - 2\mathcal{N}_0}{-\sqrt{3}\sqrt{4q^2-1} + 1 - 2q - 2\mathcal{N}_0}, \tag{43}$$

$$\kappa = \frac{1}{\sqrt{2}}\sqrt{1 + \frac{\sqrt{3}q}{2\sqrt{4q^2-1}}}, \tag{44}$$

and

$$q = \cosh\left[\tfrac{1}{3}\operatorname{arccosh}(a)\right] \tag{45}$$

with a given in Eq. (35). Note that for the singular solution $a > 1$, which corresponds to the inequality opposite to that in Eq. (31).

IV. SELF-CONSISTENT SOLUTION OF SPECTRAL PREDATOR–PREY MODEL

In this section we consider the critical question of how the coupled DW–ZF system saturates. One route to ZF saturation is through Kelvin–Helmholtz instability.[20] This approach would be appropriate in the absence of collisional

damping of ZFs. In the case of sufficient collisional damping, however, the question of the ZF saturation cannot be resolved without self-consistent determination of the DW saturation because the ZF level of turbulence should be determined by the balance between their emission from the DWs, the modulational instability of the latter on the one hand and, collisional damping of the ZFs on the other. This is the essence of the predator–prey model.

So far we have studied rather formally all possible steady DW spectra, treating their amplitude N_0 as a free parameter. Now we seek to determine the amplitude N_0 self-consistently. This can be achieved by solving Eq. (32) for the case of regular spectrum and Eq. (42) for the case of singular spectrum. The loop is closed by expressing the saturated ZF level in $\overline{D}$ through N_0 from Eq. (20). Thus, we obtain the following equation for $\mathcal{N}_0$:

$$k_0 \sqrt{\frac{\gamma^+}{\overline{D}(\mathcal{N}_0)}} = J(\mathcal{N}_0). \tag{46}$$

Here $J = J_{r(s)}$ for $\mathcal{N}_0 \leqslant \sqrt{\alpha/3}$ ($\mathcal{N}_0 > \sqrt{\alpha/3}$) and the functions $J_{r,s}$ are given by Eq. (37) and Eq. (42), respectively. The physical meaning and the form of Eq. (46) is similar to that of Eq. (25) (in which the drift wave nonlinearity was, however, neglected). The two equations constitute the balance between the drift wave generation (at the rate γ^+) and their shearing (at the rate $\overline{D}/k_0^2$). The difference in the rhs is due to the additional nonlinear damping and cascading of drift waves in Eq. (28) as compared to the quasilinear Eq. (21). It becomes important for $\mathcal{N}_0 \lesssim \sqrt{\alpha/3}$, i.e., for the regular solutions close to the separatrix and it becomes crucial for singular solutions.

To remain consistent with our model assumption about the k_r independence of the drift wave diffusivity D in Eq. (27), we calculate this quantity by averaging the right hand side of Eq. (12) over q and substitute $|\hat{\Phi}_q|^2$ from a steady state solution of Eq. (20):

$$|\hat{\Phi}_q|^2 = \frac{4\Omega_i^2 c_s^2}{L_n^2} \frac{\Sigma_{\mathbf{k}} k_r^2 \rho_s^2 (k_\theta^2 \rho_s^2)^2 \langle N\rangle^2 (1+k_\perp^2\rho_s^2)^{-4} R(\mathbf{k},q)}{\gamma_d + q^2 c_s^2 \Sigma_{\mathbf{k}} k_\theta^2 \rho_s^2 \omega_{\mathbf{k}} k_r (\partial\langle N\rangle/\partial k_r) R(\mathbf{k},q)/(1+k_\perp^2\rho_s^2)}. \tag{47}$$

We may now substitute the solution $\langle N(k)\rangle$ implicitly obtained in Sec. III B 1 into the last equation and then calculate $D_{\mathbf{k}}$ from Eq. (12). This will produce a number of complicated integrals, but in view of our simplified treatment of the drift wave spectrum $\langle N(k_r)\rangle$ we may estimate them by taking into account that $\langle N\rangle$ is a smooth function of the order of N_0 within $|k| < k_0$ domain and vanishes rapidly for $|k| > k_0$. A further simplification of the expression (47) can be made upon the observation that according to Eq. (12) the main contribution to $D_{\mathbf{k}}$ comes from reasonably large q, since $|\hat{\Phi}_q|^2$ is finite at $q=0$ [see Eq. (47)]. Thus, an estimate of $|\hat{\Phi}_q|^2$ in the interval $\gamma/V_{\rm gr} < q \leqslant q_{\max}$ suffices for our purposes. As we shall see, $|\hat{\Phi}_q|^2 \propto q^{-2}$ in this interval, so that we set $q > \gamma/V_{\rm gr}$ in Eq. (47). At this point, it is necessary to distinguish between the regular and singular spectra $\langle N(k_r)\rangle$ as described above. In the latter case, we substitute for $\langle N(k_r)\rangle \simeq N_0 (k_0/k_r)^2$ instead of N_0 in the former case. Using these approximations, Eq. (47) simplifies to

$$|\hat{\Phi}_q|^2 = \Omega_i^2 \frac{\overline{k_\theta^2}}{q^2} \frac{k_0 L}{2\pi} S N_0^2 \left(\frac{\gamma_d}{\gamma_+} - \frac{|\overline{k_\theta}| L \Omega_i^2}{8\pi k_0 V_*} S N_0 \right)^{-1}, \tag{48}$$

where $V_* = c_s^2/\Omega_i L_n$ and L denotes the radial size of the system. The factor S depends on whether the DW wave spectrum is regular (upper line) or singular (lower line)

$$S = \begin{cases} 1, & \mathcal{N}_0 \leqslant \sqrt{\alpha/3}, \\ (1/3)(k_0/k_{\min})^3, & \mathcal{N}_0 > \sqrt{\alpha/3}. \end{cases} \tag{49}$$

As a next step, we substitute the simplified expression for the zonal flow spectral mode density given by Eq. (48) into Eq. (12). Note that a formal upper boundary for the integral over q is $q \sim 1/\rho$, determined by the factor in parentheses in Eq. (12), clearly exceeds the zonal flow spectrum boundary required for the scale separation implied. At the same time, a higher order expansion in the rhs of the zonal flow generation Eq. (20) may or may not provide a cutoff of $|\hat{\Phi}_q|^2$ at a lower $q = q_{\max}$, so that it is not clear how well the zonal flow spectrum is separated from the long wavelength end of the drift wave spectrum.[14] In any case, the integral over q in Eq. (12) depends relatively weakly (linearly) upon its upper limit $q_{\max}$. Thus, from (12), we have the following simplified representation of $\overline{D}$ in Eq. (27)

$$\overline{D} = \frac{4 k_0 q_{\max} \gamma_+ S A^2 \mathcal{N}_0^2}{\Gamma - A\mathcal{N}_0} (1 + \overline{k_\perp^2}\rho_s^2) \left(1 - \frac{\overline{q^2}\rho^2}{1+k_\perp^2\rho_s^2} \right). \tag{50}$$

Here we have introduced the amplitude and damping parameters A and Γ as follows:

$$A = \frac{\overline{\kappa_\theta^2} L}{8\pi k_0} \frac{\gamma_+}{\omega_*} \frac{N_B}{\Delta\omega} \Omega_i^2, \tag{51}$$

$$\Gamma = \gamma_d / \gamma_+ . \tag{52}$$

The mean wave number of the zonal flow $\overline{q}$ arises in an obvious way from the integration of the zonal flow spectrum

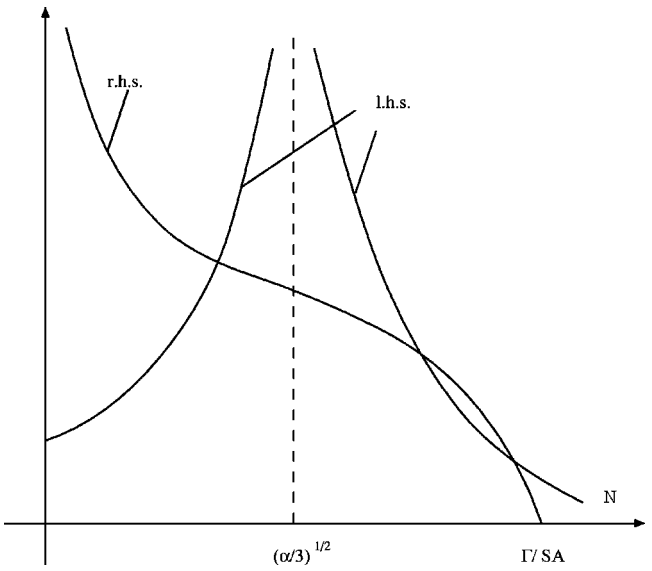

FIG. 3. Right-hand side and the left-hand side of Eq. (53). Depending on parameters, this equation has either one or three solutions.

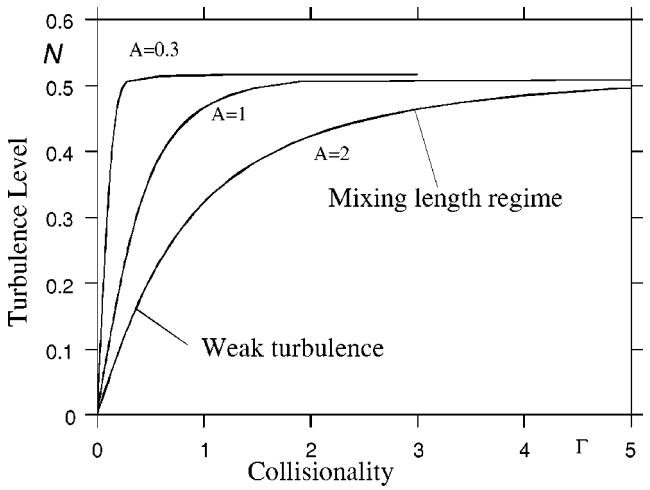

FIG. 4. The level of the drift wave turbulence $\mathcal{N}_0$ for the regular spectrum as a function of collisional damping of the zonal flows $\Gamma=\gamma_d/\gamma_+$ for different values of the amplitude parameter A. For a stronger self-nonlinearity of the drift waves (smaller A) the transition to the mixing length regime occurs faster.

over q in Eq. (12). One can neglect the dependence of $\overline{D}$ on $\overline{q}$ since $\overline{q}\rho<1$. Using the above notation, Eq. (46) can be rewritten as

$$J(\mathcal{N}_0)=\frac{\sqrt{\Gamma-SA\mathcal{N}_0}}{K\sqrt{SA}\mathcal{N}_0}, \tag{53}$$

where J is defined as in Eq. (46), whereas

$$K=2\sqrt{\frac{q_{\max}}{k_0}(1+\overline{k_\perp^2}\rho_s^2)\left(1-\frac{\overline{q}^2\rho^2}{1+k_\perp^2\rho_s^2}\right)}.$$

Our goal is to study the solutions $\mathcal{N}_0$ of Eq. (53) as a function of collisional damping rate $\Gamma=\gamma_d/\gamma^+$. As follows from Eqs. (37) and (42), the lhs of Eq. (53) is positive and has a logarithmic singularity at $\mathcal{N}_0=\sqrt{\alpha/3}$, whereas the right-hand side of this equation monotonically decreases from ∞ to 0 for $\mathcal{N}_0>0$, Fig. 3. Thus, Eq. (53) has either one (regular) solution $\mathcal{N}_0=\mathcal{N}_0(\Gamma)$ or three (one regular and two singular) such solutions, depending on the parameters K, S, and A. As may be seen from the structure of Eq. (53), it does not need to be numerically solved for $\mathcal{N}_0=\mathcal{N}_0(\Gamma)$. It is sufficient to plot the explicit dependence $\Gamma=\Gamma(\mathcal{N}_0)$ and swap the coordinates. The result is shown in Figs. 4 and 5. The three curves drawn in Fig. 4 represent the regular solution (plotted for different values of parameter A) and this solution, indeed recovers both the linear (small Γ) and the mixing length (large Γ) scalings on a universal basis. In addition to the regular solution, two other solutions emerge. One of them approaches the saturation level of the regular solution, $\mathcal{N}_0=\sqrt{\alpha/3}$ from above. The second one grows linearly with $\Gamma\gg1$ as $\mathcal{N}_0=\Gamma/SA$. Both singular solutions correspond to a condensation of the drift wave spectra at the longest radial scales. We analyze these results in more detail in the next section.

V. ANALYSIS OF THE RESULTS

The solution of the coupled drift wave–zonal flow model described in Ref. 21 and summarized in Sec. II revealed four different regimes of dynamics. Two of them may be termed ''basic drift wave–zonal flow'' regimes and the other two as condensate regimes. In all regimes the drift waves are generated by some source of free energy (as, e.g., drift wave or ITG instability) acting at relatively large radial scales. In the first of the two basic regimes, the DWs produce zonal flows but are also efficiently coupled to shorter radial scales by shearing, and are ultimately linearly damped. The second regime may be realized when the zonal flows are strongly suppressed by collisional damping and the drift waves reach such high amplitudes that local nonlinear transfer becomes important. To capture this possibility as

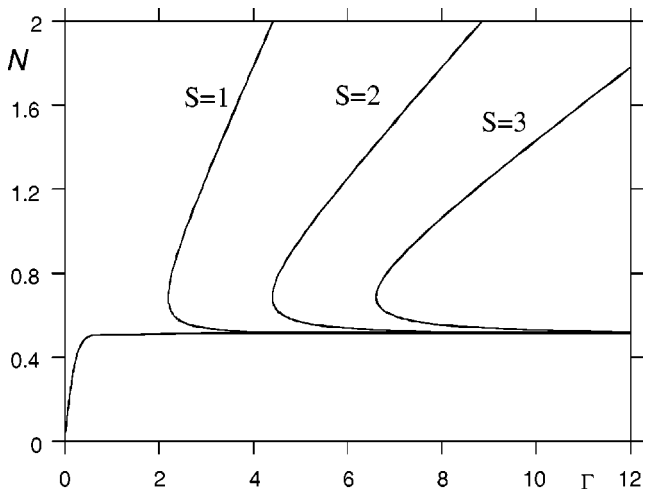

FIG. 5. The same as Fig. 4 but for both the regular and singular solutions and for different values of the cutoff parameter S and $A=0.5$. The ''condensate'' spectra (upper branches) are less likely to occur (higher damping rate of zonal flow Γ is required) if they are radially more extended (smaller $k_{\min}$, larger S).

well, the model includes a local nonlinear coupling[21] [$\Delta\omega$-term in Eq. (11)]. In very simple terms, the system operates in the first or the second basic regime depending on how the zonal flow dissipation rate is related to the drift wave generation rate, controlled by the parameter $\Gamma = \gamma_d/\gamma_+$ in Eq. (53). The turbulence level is plotted against this parameter in Fig. 4. However, the strength of the drift wave nonlinear coupling also plays a part in regime selection so that the parameter upon which the discrimination between these two regimes really depends is Γ/A (rather than Γ), with A controlling the width of the crossover in Γ between the two regimes. This may be easily seen from Fig. 4 or from the calculations in Sec. IV. Note that, in principle, the increased width of the crossover in the case of large A might be responsible for the unsaturated growth of the turbulence level with γ_d, recently observed in gyrokinetic simulations.[19,14] However, based on the bursting observed in the simulations, we discuss in Sec. VI a different explanation, which involves also the singular solution. In terms of the relevant time scales, the parameter Γ/A is proportional to

$$\frac{\Gamma}{A} \propto \frac{\gamma_d \Delta\omega}{\gamma_+^2}. \tag{54}$$

In addition to $\Delta\omega$, it depends on a few other quantities that are, however, not related to the most critical time scales exhibited in the above expression. This, together with Eq. (53), shows that if the drift waves are generated fast enough in comparison to the collisional zonal flow and nonlinear drift wave damping rates combined, i.e., $\Gamma/A \ll 1$, then their level and the associated transport scales linearly with the zonal flow damping, i.e.,

$$\mathcal{N}_0 \simeq \frac{\Gamma}{A}. \tag{55}$$

In the opposite case, when $\Gamma/A \gg 1$, Eq. (53) can be satisfied only if its lhs is close to the singularity at $\mathcal{N}_0 = \sqrt{\alpha/3}$. Thus, for large Γ/A the drift wave amplitude saturates at this level, and takes the following asymptotic form:

$$\mathcal{N}_0 \simeq \sqrt{\alpha/3}\left[1 - \frac{3}{4}\,\frac{\sqrt{3}-\sqrt{1+2\sqrt{\alpha/3}}}{\sqrt{3}+\sqrt{1+2\sqrt{\alpha/3}}} \times \exp\left(-\frac{1}{KA}\sqrt{\sqrt{\alpha/3}\Gamma - A}\right)\right]. \tag{56}$$

Both asymptotic regimes are apparent in Fig. 4, where $\mathcal{N}_0$ is plotted against Γ (rather than Γ/A, which would formally minimize the number of parameters involved) but for different values of A. The reason is that $\Gamma = \gamma_d/\gamma_+$ is usually known better than A, since the latter depends on $\Delta\omega$, which is merely parametrized here. Note that in addition to Γ/A, the solution of Eq. (53) depends also on the parameter $K\sqrt{A}$ that contains another somewhat uncertain parameter, namely $q_{\max}$. However, it may be seen from Eq. (53) and Fig. 3 that the existence of the two basic regimes corresponding to the linear dependence of $\langle N\rangle$ upon γ_d with subsequent saturation, remain independent of the concrete values of the parameters $\Delta\omega$ and $q_{\max}$. (There always exists at least one root at $\mathcal{N}_0 < \sqrt{\alpha/3}$.) As for the $q_{\max}$, however, we can safely set $q_{\max} \lesssim k_0$ (Ref. 19) since $V_{gr}q < \omega_{\mathbf{k}}$. It should be also noted that the dependence on the remaining control parameter, $\alpha = \gamma_+/(\gamma_+ + \gamma_-)$ is rather weak. This parameter is clearly of a somewhat artificial origin and relates the $\gamma(k)$ to its replacement, the "box" function (26). This is an approximation which requires more detailed investigation.

First, the scaling $\mathcal{N}_0 \propto \Gamma/A$ remains valid also for continuous $\gamma(k)$. This may be seen by substituting the expression for $\overline{D}$ in Eq. (50) [or its obvious analog for continuous $\gamma(k)$] into Eq. (25), since the quasilinear approximation of Sec. III A is valid for small Γ, where linear scaling is applicable. Turning to the strongly nonlinear regime, in which the WKB solution of Sec. III A is inapplicable in its present form, one may notice the following. In this case, the solution follows the separatrix in Fig. 1, and within the region of positive γ stays close to the fixed point (see Fig. 2). This is basically the limit of small $\overline{D}$ in Eq. (28), which exemplifies the problem of singular perturbation for an arbitrary $\gamma(k_r)$. The solution can also be found in this limiting case by constructing a "central manifold" (e.g., Ref. 33), which is the solution of Eq. (28) with $\overline{D}=0$ and in which the hyperbolic point on the phase portrait, Fig. 1, follows the slowly (on the "time-scale" $\delta k_r \sim \sqrt{\overline{D}/\gamma}$) varying function $\gamma(k_r)$. Thus, the solution stays close to the central manifold which is simply $\langle N(k_r)\rangle = \gamma(k_r)N_B/\Delta\omega$, where $\gamma(k_r) \geqslant 0$ and $\langle N\rangle = 0$ where $\gamma(k_r) < 0$.

The further treatment of Eq. (28) from the perspective of the theory of dynamical systems brought up a new class of solutions which also approach the separatrix in Fig. 1, but from the outside. In terms of their k_r dependence these are singular solutions that branch off at some critical value of $\Gamma = \Gamma_1$ on the bifurcation diagram in Fig. 5. There are two branches of singular solutions for each set of parameters. The lower branch asymptotically approaches the (unique) regular solution when the parameter $\Gamma \to \infty$ (or $\overline{D} \to 0$). Since, in this parameter regime, both solutions are close to the separatrix they stay at the hyperbolic point within an extended interval of k_r, i.e., see Fig. 1, close to each other. As may be seen from, e.g., Eq. (28), the hyperbolic point $\langle N\rangle = \gamma^+ N_B/\Delta\omega, d\langle N\rangle/dk_r = 0$ corresponds to the equilibrium between linear instability of the drift waves and their nonlinear damping, while the role of their scattering in k_r by the zonal flows is relatively minor. The process of scattering in k_r, however, enters the problem (28) (via the k_r space diffusion term) as a singular perturbation and may thus become important no matter how small it is. Namely, the singular solution being outside the separatrix cannot satisfy the critical balance condition $\langle N(k_r)\rangle = \gamma(k_r)N_B/\Delta\omega$ for all k_r, and thus diverges from its regular counterpart at small k_r. In other words, the drift waves accumulate at $k_r = 0$. This corresponds to the process of drift wave condensation. The spectral shape of this solution at the singularity ($k_r \to 0$) is determined by the balance of the nonlinear and diffusion terms of Eq. (28), i.e., $\langle N\rangle \propto 1/k_r^2$ as may also be seen from the general solution (32). It is interesting to note that con-

densation, is due to k_r diffusion as is shearing, yet it leads to the singularity at $k_r=0$. In contrast to shearing, condensation is only possible when diffusion works in concert with nonlinearity. Such competition and condensation occur only for concave spectra.

Note, however, that this behavior of the spectrum at the origin is not universal for the drift wave condensation but rather results from our particular representation of the nonlinear coupling and refraction processes. At the same time the diffusive approximation and quadratic nonlinearity that are employed here is not an artificial choice. More importantly, the balance between the terms that both saturate the turbulence in the case of regular spectrum makes connection to the long scale reservoir (condensate) of turbulence energy. It should be also noted that the scale invariant behavior of the singular solution results from the symmetry of Eq. (28) in the corresponding parameter range (where the linear instability term can be neglected). For example, on the lower singular branch and for sufficiently large Γ, where $\overline{D}\propto N^2$, Eq. (28) is invariant under the transformation $k_r\rightarrow\alpha k_r$, $\langle N\rangle \rightarrow\alpha^2\langle N\rangle$. Since $\overline{D}$ depends on N as on a functional, the scale invariance survives also for smaller Γ and for the upper singular branch, provided that the linear instability term can be neglected. This may be useful for the analysis of the transport scaling from the perspective of self-organized criticality, as it was demonstrated by the authors of Refs. 34 and 35. In particular, their detailed discussion of the relation between the Bohm scaling of transport, the scale invariance, the infrared catastrophe (condensate), and thus the role of the global system size in the Bohm transport regime appears to be applicable to the condensate solution discussed in this paper.

To summarize the above analysis, starting from some critical value of the damping rate $\Gamma=\Gamma_1$, two additional solutions $N_0(\Gamma)$ emerge, as shown in Fig. 5. The critical value Γ_1 (see Fig. 5) depends on the parameters A, S, and K in a way that may be understood from the formula (53), as well as from a few examples given in Fig. 5. The multiplicity of solutions is, of course, quite typical for nonlinear dynamical systems. Usually, the first step in mapping the branch selection consists of a stability analysis. A ''rule of thumb'' (obvious for systems reducible to first order ODE's in time) is that for the fixed values of parameters, stable branches must intermingle with unstable ones. We have three branches here and the lowermost should be stable, at least for small Γ. This is verified below.

A. Stability analysis

In the parameter regime $\mathcal{N}_0\propto\Gamma\ll 1$, we may restrict ourselves to a straightforward analysis of the quasilinear solution of Sec. III A. Upon Laplace transformation of Eq. (11), or, equivalently, replacing $\partial\langle N\rangle/\partial t$ by $\lambda\langle N\rangle$ instead of Eq. (21) we arrive at the following eigenvalue problem:

$$\frac{\partial}{\partial k_r}D_{\mathbf{k}}\frac{\partial\langle N\rangle}{\partial k_r}+(\gamma_{\mathbf{k}}-\lambda)\langle N\rangle=0. \tag{57}$$

The steady state solution described by the asymptotic formula (23) discussed in Sec. III A is thus an eigenfunction of the problem (57) with the eigenvalue $\lambda=0$ and, by construction, it corresponds to the ''lowest level'' (the eigenfunction with no zeroes) in the potential well formed by the function $\gamma(k_r)$. Using a quantum-mechanical analogy, the value $\lambda=0$, corresponds to the lowest energetic level $E_0=-\lambda=0$, of the oscillator with the potential given by $\gamma_{\mathbf{k}}$. All other energetic states have, therefore, positive energies $E_n>0$, so that the λ-spectrum is on the left half-axis and the steady state solution of Eq. (11) is stable. The eigenvalues $\lambda_n<0$ may be found from Eq. (24) with an obvious replacement $\gamma\rightarrow\gamma-\lambda$. It should be mentioned, however, that the diffusion coefficient $D_{\mathbf{k}}$ depends on the steady state solution $\langle N\rangle=\langle N\rangle_0$, via a functional. This will slightly change the above stability analysis but will not change the conclusion about the stability of the steady state solution found in the linear approximation in Sec. III A.

Moving to higher Γ on the same branch of the solution $N(\Gamma)$, i.e., when the solution becomes nonlinear and the $\Delta\omega$-term in Eq. (11) becomes increasingly important, we observe that a linear stability analysis produces the following spectral problem for the perturbation $\delta\langle N\rangle$ [instead of that given in Eq. (57)]

$$\frac{\partial}{\partial k_r}D_{\mathbf{k}}\frac{\partial}{\partial k_r}\delta\langle N\rangle+\left(\gamma_{\mathbf{k}}-\lambda-2\Delta\omega\frac{\langle N\rangle_0}{N_B}\right)\delta\langle N\rangle=0. \tag{58}$$

The additional (negative definite) term here makes the potential well shallower and narrower as compared to Eq. (57). Therefore, λ needs to be decreased in order to compensate for this additional term and preserve the eigenfunction. This clearly shifts the λ-spectrum to the left, thus producing a stabilizing effect on the nonlinear steady state solution $\langle N\rangle_0$.

Turning to the singular spectrum we note that even though its lower branch may be very close to the regular spectrum (when both approach the separatrix), its stability analysis must be intrinsically different from that of the regular solution. First of all the differential operator in Eq. (58) must be defined on an extended functional space that includes functions which are nonintegrable at $k_r=0$. Also the last term in the parentheses is now singular in k_r, since $\langle N\rangle_0\propto 1/k_r^2$ for singular solutions. Leaving aside, however, the stability analysis of the two singular branches, we rely on the simple rule of stability alternation mentioned above. Based on the established stability of the regular branch, there is a good reason to expect that the nearest to it, i.e., the lower singular branch is unstable whereas the next one, i.e., the upper one, should again be stable.

B. Inverse bifurcation

As may be seen from Eq. (46), the two lower branches of its solution merge at $\Gamma=\infty$, Fig. 5, taking the value $\mathcal{N}_0=\sqrt{\alpha/3}$ (see also Fig. 3). This behavior originates from the separatrix solution (an orbit with infinite period) of the dynamical system given by Eq. (28), which corresponds to the singularity of the function $J(\mathcal{N}_0)$ in Eq. (46) at $\mathcal{N}_0=\sqrt{\alpha/3}$ (the period diverges on the separatrix). This singularity actually ensures the existence of these two solutions for all $\Gamma>\Gamma_1$. The function $J(\mathcal{N}_0)$, however, will become regular if the separatrix solution is destroyed by a perturbation not included in our analysis of Eq. (46). One can think of a phe-

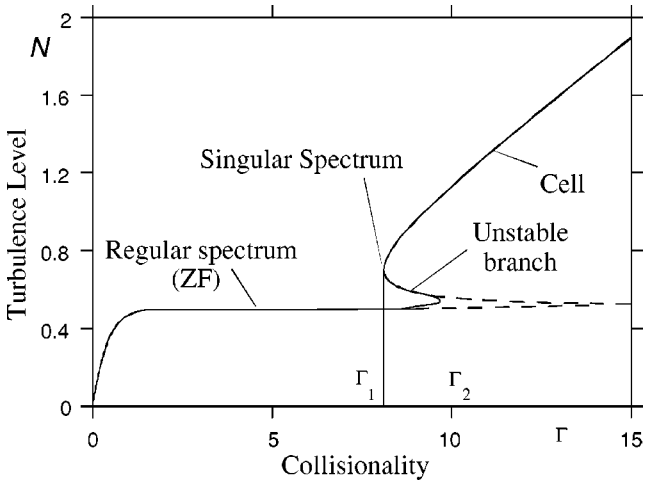

FIG. 6. The solution for the drift wave amplitude in the case of perturbed Eq. (27) (see text) giving rise to inverse bifurcation related to a second critical $\Gamma=\Gamma_2$.

nomenon similar to the separatrix splitting or formation of stochastic layers around them, well known in the theory of dynamical systems, e.g., Ref. 33. Such a perturbation may easily appear in Eq. (28) if we treat the coefficients more realistically, e.g., as some functions of k_r, or add random noise to this equation. This should create a peak of a final height on the $J(\mathcal{N}_0)$ graph at $\mathcal{N}_0=\sqrt{\alpha/3}$ and, as may be understood from Fig. 3, these two branches should merge at some $\Gamma_2<\infty$, as shown in Fig. 6.

The overall bifurcation diagram, shown in Fig. 6, thus takes the classical form of an *S*-type bifurcation diagram. The region $\Gamma<\Gamma_1$ is where the zonal flow regime should be expected, whereas at $\Gamma>\Gamma_2$, only a condensate spectrum is possible. Note that after this bifurcation the spectrum substantially increases in intensity and should thus become broader in k_θ, although we admittedly neglected the spectral evolution in k_θ in favor of its more important dependence on k_r. The condensate type scaling in k_r, $\langle N\rangle\propto 1/k_r^2$ will also spread with growing Γ (and thus with the drift wave intensity) over larger k_r [which may be seen from Eqs. (28) and (53)], so that the spectrum will lack the k_r scale, imposed at smaller amplitudes by the characteristic scale of $\gamma_{\mathbf{k}}$. In the intermediate domain $\Gamma_1<\Gamma<\Gamma_2$, both the ZF and condensate solutions are possible and they are connected by the (presumably) unstable branch of the stationary solution. Due to slow variations of the system parameters (as e.g., temperature or density gradient variation, caused by transport) the parameter Γ as well as its critical values $\Gamma_{1,2}$ also change and the system may leave the intermediate domain $\Gamma_1<\Gamma<\Gamma_2$. Then, only one solution remains possible, to which the system must transit unless it was already realized in the intermediate domain.

VI. SUMMARY AND DISCUSSION

In this paper we have considered various turbulence regimes that are likely to occur in a coupled drift wave–zonal flow system. The primary focus was on turbulence saturation and on the dependence of its level on the flow damping (ion collisionality) γ_d. This study revealed a rather complicated dependence of the turbulence spectrum structure to governing parameters. The principal results of this paper are the following:

(i) In the limit of weak zonal flow damping, $\gamma_d\Delta\omega/\gamma^2\ll 1$, the DW turbulence level (and thus transport) scales with collision rate as $N_0\propto\gamma_d/\gamma$, where $\Delta\omega$ is the nonlinear damping of drift waves and γ is their linear growth rate.

(ii) In the opposite limit of strong collisional damping of ZFs ($\gamma_d\Delta\omega/\gamma^2\gg 1$), drift waves saturate at a level independent of collisionality which is roughly consistent with mixing length predictions. Crossover occurs at $\gamma_d\Delta\omega/\gamma^2\sim 1$. This behavior is robust, the solution is linearly stable, and no turbulent viscosity needs to be assumed for saturation.

(iii) Starting from a critical $\gamma_d=\gamma^+\Gamma_1$ (see Fig. 6), two new solutions branch off. They manifest a ZF induced inverse energy transfer within the DW component of turbulence. They have significantly higher level of turbulence and transport. Their spectral behavior at $k_r\to 0$ is that of a condensate type (i.e., a cutoff $k_r=k_{\min}$ required since $\langle N\rangle\propto k_r^{-2}$), but the corresponding spatial structures lack a characteristic scale in k_r and have $k_\theta>k_r$ but not $k_\theta\gg k_r$.

These findings merit further comments. First of all, in a certain parameter range, more than one turbulent state may exist. Nevertheless, the relevant stability analysis allowed us to identify the lowermost branch of the solution (which tracks γ_d and ultimately saturates) with a clearly generic response of the self-regulated drift wave–zonal flow system to the collisional self-damping γ_d. The change of the turbulence regime occurs (approximately) when the parameter $\gamma_d\Delta\omega/\gamma_+^2$ exceeds unity, manifesting a situation in which the zonal flows are not excited and the drift waves saturate via nonlinear damping, $\langle N\rangle\propto\gamma/\Delta\omega$. The saturated drift wave spectrum on this branch is regular in k and stable. For a simple model of linear instability and nonlinear damping of the drift waves, we were able to calculate the wave spectral density $\langle N\rangle$ in a closed form that has the aforementioned behavior.

In addition to the solution regular in k_r there are two singular solutions with higher $\langle N\rangle$ that branch off at sufficiently strong zonal flow damping γ_d. It is interesting to note that conditions under which the spectral condensate in k_r should form (strong damping of zonal flows) are also intrinsically favorable to the development of radially extended cells or streamers. Conversely, when the zonal flows are not strongly suppressed, they should restrict cell formation via shear-enhanced decorrelation. We summarize our thoughts on the condensate and cells, below.

(1) Radially extended cells require strong suppression of ZFs, i.e., well developed cells and ZFs do not co-exist.

(2) The γ_d-threshold for cells is very sensitive to $k_{\min}\sim 1/l_{\text{cell}}$. Note that this suggests that flux tube and full geometry simulations may arrive at different results. Formation of systemwide cells would require strong damp-

ing of ZFs. This may be easily seen from Fig. 5 and from the definition of S for the singular spectrum in Eq. (49): larger S (smaller $k_{\min}$) require larger γ_d.

(3) The onset of the cell regime should not necessarily be accompanied by a significant shift of the DW spectrum to smaller k_r. Due to the increased role of the DW nonlinearity, the spectral broadening is a competing and regulatory process in this regime.

(4) Based on bifurcation diagrams derived from our results (i.e., Fig. 6) *bursting* may appear as a hysteresis loop phenomenon, i.e., transitions between the zonal flow dominated (i.e., regular) and condensate solutions can occur.

It is worthwhile to comment on the last issue. In general, the S-type bifurcation diagram is indeed suggestive of hysteretic bursting behavior of the underlying dynamical system. However, one needs to complement this formally quasistatic picture with the feedback from each state to which the system moves, so that the reverse transition would be possible as well. For example, suppose the thermal transport gradually reduces the ITG growth rate γ^+, so that the system proceeds slowly along the lower branch on Fig. 6 towards $\Gamma \equiv \gamma_d/\gamma^+ = \Gamma_2$ and must then jump to the upper (cell) branch. After this transition, new phenomena should come into play. First of all, the spatial structure of the cell also suggests strong shearing of turbulence, but this time in the radial direction,[22] so that the dynamical equation (11) should be supplied for a diffusion term in k_θ rather than in k_r. The relevant equations have been derived recently in Ref. 22. Another possibility is to rightshift the critical point Γ_1 on Fig. 6 due to condensation at $k_r=0$, since the Γ_1 sharply increases with decreasing $k_{\min}$, as seen from Fig. 5. This will force the system to return to the lower branch and the process may thus repeat.

Phenomena similar to the proposed cyclic bifurcations between these two states have recently been observed in simulations.[19] Evidently, under these circumstances, neither of the branches of stationary solutions fully captures the scaling of transport (or turbulence level $\langle N\rangle$) with the collisionality γ_d. However, one can speak of a weighted (time averaged) mixture of states for which such a scaling can be unambiguously defined. This has been inferred from gyrokinetic simulations and yielded $\chi_i \propto \gamma_d^{0.75}$. This is not inconsistent with the diagrams in Figs. 5 and 6 as being between the upper branch (that scales asymptotically as γ_d) and the lower one (which saturates with γ_d). Note, however, that the predator–prey model described in this paper reproduces bursting dynamics within only the regular branch of the solution.[24]

A final remark should be made on the linear scaling of $\langle N\rangle$ with γ_d where the DW turbulence level formally vanishes as $\gamma_d \to 0$. Clearly, our initial assumption (see Sec. II A) about an approximate balance between the linear generation of the DWs and their nonlinear decorrelation becomes invalid in this limit. The balance here is really between the DW linear generation and their shearing by self-generated ZFs. The excitation of the latter has, generally speaking, its own threshold so that the limiting case of very small γ_d needs to be addressed separately. This has been the subject of an accompanying paper.[23] For the applications to the subject of the present paper, it is important to note that the threshold becomes significant for broad drift wave spectra since it scales as $N_{\rm th} \sim \Delta k^2 \rho_s^4 L_n^{-2}$ with the spectrum width $\Delta k \rho_s \leqslant 1$. Also, zonal flow saturation mechanism based on a generalized Kelvin–Helmholtz instability has been considered recently in Ref. 20.

ACKNOWLEDGMENTS

We thank S. Champeaux, M. N. Rosenbluth, A. Smolyakov, T. S. Hahm, Z. Lin, and F. L. Hinton for interesting discussions.

This research was supported by the U.S. Department of Energy, Grant No. FG03-88ER53275.

[1] G. Schubert and J. A. Whitehead, Science **163**, 71 (1969).
[2] F. H. Busse and A. C. Orr, J. Fluid Mech. **166**, 173 (1986).
[3] A. C. Orr and F. H. Busse, J. Fluid Mech. **174**, 313 (1987).
[4] W. Horton, Rev. Mod. Phys. **71**, 735 (1999).
[5] P. W. Terry, Rev. Mod. Phys. **72**, 109 (2000).
[6] P. H. Diamond *et al.*, in *Plasma Physics and Controlled Nuclear Fusion Research*, 15th IAEA Fusion Energy Conference, Seville, Italy, 1994 (International Atomics Energy Agency, Vienna, 1996), p. IAEA-CN-60/D-13, p. 323.
[7] A. Hasegawa and M. Wakatani, Phys. Rev. Lett. **59**, 1581 (1987).
[8] G. Hammet, M. Beer, W. Dorland, S. C. Cowley, and S. A. Smith, Plasma Phys. Controlled Fusion **35**, 973 (1993).
[9] M. A. Beer, Ph.D. thesis, 1995.
[10] B. Scott, Plasma Phys. Controlled Fusion **34**, 1977 (1992).
[11] Z. Lin, T. S. Hahm, W. W. Lee, W. M. Tang, and R. B. White, Science **281**, 1835 (1998).
[12] A. M. Dimits, G. Bateman, M. A. Beer *et al.*, Phys. Plasmas **7**, 969 (2000).
[13] R. D. Sydora, V. K. Decyk, and J. M. Dawson, Plasma Phys. Controlled Fusion **38**, A281 (1996).
[14] T. S. Hahm, M. A. Beer, Z. Lin, G. W. Hammett, W. W. Lee, and W. M. Tang, Phys. Plasmas **6**, 922 (1999).
[15] S. Coda, M. Porkolab, and K. H. Burrell, Phys. Lett. A **273**, 125 (2000).
[16] K. H. Burrell, Phys. Plasmas **6**, 4418 (1999).
[17] M. N. Rosenbluth and F. L. Hinton, Phys. Rev. Lett. **80**, 724 (1998).
[18] F. L. Hinton and M. N. Rosenbluth, Plasma Phys. Controlled Fusion **41**, A653 (1999).
[19] Z. Lin, T. S. Hahm, W. W. Lee, W. M. Tang, and P. H. Diamond, Phys. Rev. Lett. **83**, 3645 (1999).
[20] B. Rogers, W. Dorland, and M. Kotschenreuther, Phys. Rev. Lett. **85**, 5336 (2000).
[21] P. H. Diamond, M. N. Rosenbluth, F. L. Hinton, M. Malkov, J. Fleischer, and A. Smolyakov, in *Plasma Physics and Controlled Nuclear Fusion Research*, 17th IAEA Fusion Energy Conference, Yokohama, Japan, 1998 (International Atomics Energy Agency, Vienna, 1998), p. IAEA-CN-69/TH3/1.
[22] P. H. Diamond *et al.*, in *Plasma Physics and Controlled Nuclear Fusion Research*, 17th IAEA Fusion Energy Conference, Sorrento, Italy, 2000 (International Atomics Energy Agency, Vienna, 2000), IAEA-CN-77/ (to be published).
[23] M. A. Malkov, P. H. Diamond, and A. Smolyakov, Phys. Plasmas **8**, 1553 (2001).
[24] M. A. Malkov, P. H. Diamond, and M. N. Rosenbluth (unpublished).
[25] P. H. Diamond, Y.-M. Liang, B. A. Carreras, and P. W. Terry, Phys. Rev. Lett. **72**, 2565 (1994).
[26] P. H. Diamond, V. B. Lebedev, D. E. Newman, and B. A. Carreras, Phys. Plasmas **2**, 3685 (1995).
[27] W. Horton, G. Hu, and G. Laval, Phys. Plasmas **3**, 2912 (1996).
[28] B. Galperin, S. Sukoriansky, and H.-P. Huang, Phys. Fluids **13**, 1545 (2001).
[29] P. Beyer, S. Benkadda, X. Garbet *et al.*, Phys. Rev. Lett. **85**, 4892 (2000).

[30]N. Mattor and P. H. Diamond, Phys. Plasmas **1**, 4002 (1994).
[31]A. I. Smolyakov, P. H. Diamond, and V. I. Shevchenko, Phys. Plasmas **7**, 1349 (2000).
[32]M. V. Fedoryuk, *Asymptotic Methods for Linear Differential Equations* (Nauka, Moscow, 1983) (in Russian).
[33]J. Guckenheimer and P. Holmes, *Nonlinear Oscillations, Dynamical Systems, and Bifurcations of Vector Fields* (Springer-Verlag, New York, 1983).
[34]P. H. Diamond and T. S. Hahm, Phys. Plasmas **2**, 3640 (1995).
[35]T. Hwa and M. Kardar, Phys. Rev. A **45**, 7002 (1992).